

## Antisolvent Precipitation of Vitamin B<sub>6</sub>: A Thermodynamic Study

I. Kikic,<sup>\*,†</sup> N. De Zordi,<sup>‡</sup> M. Moneghini,<sup>‡</sup> and D. Solinas<sup>†</sup>

<sup>†</sup>Department of Industrial Engineering and Information Technology, University of Trieste, Via Valerio 10, 34127 Trieste, Italy

<sup>‡</sup>Department of Chemical and Pharmaceutical Sciences, University of Trieste, Via Giorgieri 1, 34127 Trieste, Italy

**ABSTRACT:** A supercritical antisolvent precipitation process was applied to recrystallize vitamin B<sub>6</sub> from ethanol solution in CO<sub>2</sub>. By means of the Peng–Robinson equation of state (PR EoS), we performed preliminary studies to identify better operative conditions in terms of the organic solvent, pressure, temperature, and ability to carry a precipitate of the solute. This simulation was also considered to estimate the vitamin B<sub>6</sub> particle size starting from supersaturation conditions.

### INTRODUCTION

Vitamin B<sub>6</sub> (3-hydroxy-4,5-bis(hydroxymethyl)2-methylpyridine), also named pyridoxine, is one of eight water-soluble B vitamins. The B vitamins help the body to convert carbohydrates into glucose, which is burned to produce energy. These vitamins are often referred to as the B complex and are essential in the metabolism of fats and protein. B complex vitamins play an important role in maintaining muscle tone in the gastrointestinal tract and promoting the health of the nervous system, skin, hair, eyes, mouth, and liver. Pyridoxine is an important vitamin for maintaining healthy nerve and muscle cells, and it aids in the production of DNA and RNA. Vitamin B<sub>6</sub> is necessary for proper absorption of vitamin B<sub>12</sub> and for the production of red blood cells and cells of the immune system.<sup>1</sup>

The modification of vitamin B<sub>6</sub> morphology to influence its absorption and dissolution is of interest since it can determine the variation of the suggested quantity per diem to be assumed. Recently<sup>2</sup> the vitamin was incorporated with montmorillonite to modify its release.

This work concerns the mechanism of antisolvent precipitation (or crystallization) using supercritical carbon dioxide (SCO<sub>2</sub>). The major advantage of SCO<sub>2</sub> is that it can be efficiently separated, by decompression, from both organic cosolvents and solid products, making the single step process easier, but the low solubility of the majority of polar and ionic drug in CO<sub>2</sub> limits its use as pure solvent media. Alternative approaches to solve this problem are proposed by combining CO<sub>2</sub> with an organic solvent characterized by solvating properties. The expansion degree of the organic solvent modulated by the CO<sub>2</sub> content in the mixture offers different opportunities for the development of a suitable methodology for the processing of the materials, such as precipitation (DELOS, GAS, and SAS).<sup>3–5</sup>

In particular, supercritical fluid (SCF) process operating parameters can be adjusted to vary supersaturation and conditions for nucleation and crystal growth across a wide range.

Antisolvent precipitation processes can be successfully applied for the modification of the morphology of drugs or for the preparation of composites with pertinent release properties.<sup>3</sup>

In this paper preliminary results are reported for the choice of the appropriate experimental conditions for the supercritical antisolvent precipitation of vitamin B<sub>6</sub>. Particular attention is

**Table 1. Experimental Mole Fraction Solubilities  $x$  of Vitamin B<sub>6</sub> in the Considered Organic Solvents at Temperature  $T$  and Pressure  $P = 0.1$  MPa<sup>a</sup>**

solvent	$T/K$	$10^2 x$
acetone	298	0.127
	308	0.131
	310	0.135
	313	0.136
methanol	298	1.585
	308	2.447
	310	2.468
	313	2.517
ethanol	298	0.363
	308	0.380
	310	0.384
	313	0.396
THF	298	0.240
	308	0.249
	310	0.253
	313	0.271

<sup>a</sup> Standard uncertainties  $u$  are  $u(T) = 0.1$  K,  $u(P) = 0.05$ ,  $u(x) = 0.03$ .

also given to the mechanism of crystallization by means of the screw dislocation equation.

### EXPERIMENTAL SECTION

**Materials and Methods.** The vitamin B<sub>6</sub> (purity  $\geq 0.98$  molar fraction) was purchased from Sigma Aldrich (Italy). All of the organic solvents (tetrahydrofuran, THF; acetone; ethanol, EtOH and methanol, MeOH) were of analytical grade and were

**Special Issue:** Kenneth N. Marsh Festschrift

**Received:** August 4, 2011

**Accepted:** October 4, 2011

**Published:** October 20, 2011

Table 2. Pure Component Properties

compound	$M_w$	$T_c$	$P_c$	$\omega$	$T_{fus}$	$\Delta_{fus}H(T_{fus})$	$V^s$	$V^l$
	$g \cdot mol^{-1}$	K	MPa		K	$kJ \cdot mol^{-1}$	$cm^3 \cdot mol^{-1}$	$cm^3 \cdot mol^{-1}$
vitamin B6	169.18	714.5 <sup>a</sup>	3.83 <sup>a</sup>	1.71 <sup>a</sup>	433.18 ± 0.2 <sup>b</sup>	31.15 ± 0.5 <sup>b</sup>	142.06 <sup>c</sup>	175 <sup>d</sup>
CO <sub>2</sub>	44.01	304.1	7.38	0.24				
acetone	58.08	508.1	4.70	0.30				
methanol	32.04	512.58	8.10	0.56				
ethanol	44.06	516.15	6.37	0.64				
THF	72.11	540.20	5.19	0.24				

<sup>a</sup> Calculated with the procedure described in ref 7 (Lydersen's group contribution method). <sup>b</sup> This work (DSC experimental data). <sup>c</sup> Calculated from the volume of the crystal cell. <sup>d</sup> Calculated with Girolami's method.<sup>9</sup>

provided by J.T. Baker (Netherlands). The CO<sub>2</sub> (purity 0.99 molar fraction) was supplied by SIAD (Italy).

**Determination of Vitamin Solubility in Organic Solvents.** Vitamin B<sub>6</sub> solubility (Table 1) in the considered organic solvents was measured at 298 K, 308 K, 310 K, and 313 K. A weighed amount of the drug was added to 10 mL of solvent under stirring until turbidity was observed. After one hour, the solutions were then filtered, and 1  $\mu$ L of each one was diluted in the selected solvent. The concentration is then evaluated spectrophotometrically (Thermo Scientific Evolution 60 S, USA). Each experiment was carried out in triplicate (coefficient of variation (CV < 3 %) as reported from Kikic et al.<sup>6</sup>

**Differential Scanning Calorimetry (DSC).** The melting temperature ( $T_{fus}$ ) and enthalpy of fusion ( $\Delta_{fus}H(T_{fus})$ ) were measured by means of DSC mod. TA 4000 (Mettler, Greifensee, Switzerland), equipped with a measuring cell DSC 20. A fixed amount of vitamin B<sub>6</sub> (1 mg) was placed in a pierced aluminum crucible and heated at a scanning rate of 5 K  $\cdot$  min<sup>-1</sup> from (303 to 470) K under air atmosphere. The equipment was calibrated using indium as a standard. Each experiment was carried out in triplicate.

**Vitamin Precipitation.** The detailed experimental equipment used in the antisolvent precipitation experiments has been already presented by Kikic et al.<sup>7</sup> A precipitation vessel with a capacity of 50 mL was loaded with a 7 mL solution of vitamin B<sub>6</sub> in the organic solvent. The supercritical CO<sub>2</sub> was added from the bottom of the chamber, and when the liquid phase expanded, the formed particles were retained in the vessel by a suitable filter. During the coprecipitate formation, the temperature was fixed at 298 K and 313 K and the pressure was set at 5.5 MPa and 7.2 MPa, respectively. Precipitation experiments were carried out in triplicate.

**Solubility Calculations.** The knowledge of the vitamin B<sub>6</sub> solubility as a function of the solvent and antisolvent composition is essential to establish the correct experimental conditions for the antisolvent precipitation process. The phase equilibrium of pure solid (component 3) in a solution of composition  $x_3$  can be described by the following equilibrium equation:

$$f_3^S(T, P) = x_3 \cdot \hat{\phi}_3^L \cdot P \quad (1)$$

where  $\hat{\phi}_3^L$  is the fugacity coefficient of the solute in the solution (pure liquid solvent or liquid solvent plus CO<sub>2</sub> antisolvent) and  $P$  is the pressure of the system (5.5 MPa and 7.2 MPa).

The fugacity coefficient of the pure solid,  $f_3^S(T, P)$ , can be calculated from that of the pure liquid  $f_3^L(T, P)$  as reported by ref 8.

Table 3. Binary Interaction Parameters Calculated by the PR EoS

system	T/K	10 <sup>2</sup> $k_{ij}$	10 <sup>2</sup> $l_{ij}$	ref		
CO <sub>2</sub>	THF	298	0.70	0.07	12	
		313	0.08	0.19	12	
	acetone	298	2.05	1.42	13	
		313	2.14	2.93	13	
	EtOH	298	6.45	3.17	13	
		313	8.62	-0.39	13	
	MeOH	298	7.33	2.92	14	
		313	7.78	1.59	14	
	Vitamin B6	CO <sub>2</sub>		-0.07		this work
			THF	298	-0.28	
		308		1.15		this work
		310		1.42		this work
313		1.71			this work	
acetone		298	-0.014		this work	
		308	1.54		this work	
		310	1.80		this work	
		313	2.31		this work	
MeOH		298	0.32		this work	
		308	0.28		this work	
		310	0.45		this work	
		313	1.71		this work	
EtOH		298	2.55		this work	
		308	3.57		this work	
		310	3.79		this work	
		313	4.08		this work	

The melting point and heat of fusion were determined by a differential scanning calorimeter, while molar solid and liquid volumes ( $v_3^S$ ,  $v_3^L$ ) were calculated by crystal unit cell data and Girolami's method,<sup>9</sup> respectively.

The study applied the Peng–Robinson equation of state (PR EoS) that was used for the calculation of the fugacity coefficient in the solution  $\hat{\phi}_3^L$  with the classical van der Waals mixing rules.  $a$  and  $b$  are energetic and volumetric parameters containing two binary interaction parameters:  $k_{ij}$  for the attractive term and  $l_{ij}$  for the repulsive term.

Pure component properties used in the equation of state are reported in Table 2. The critical properties such as critical

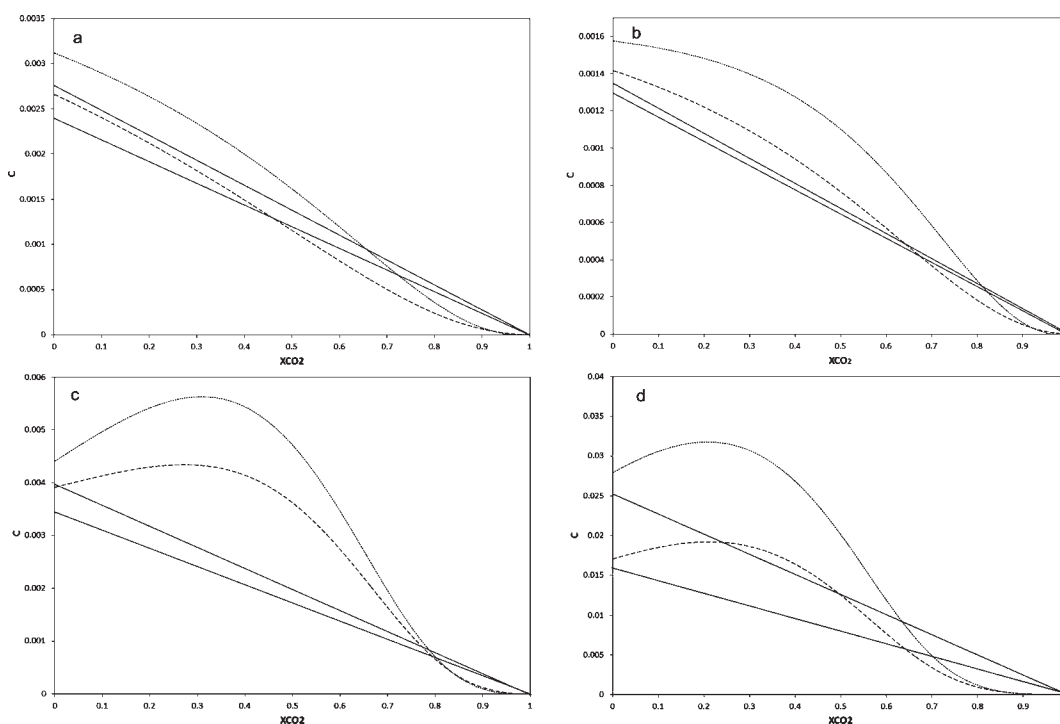


**Figure 1.** Vitamin B<sub>6</sub> solubility behaviors in ternary systems with THF–CO<sub>2</sub> (a), acetone–CO<sub>2</sub> (b), EtOH–CO<sub>2</sub> (c), and MeOH–CO<sub>2</sub> (d). The dashed line refers to the systems at temperature  $T = 298$  K and pressure  $P = 5.5$  MPa. The dotted line refers to the systems at  $T = 313$  K and  $P = 7.2$  MPa. The solid lines refer to ideal dilution evolution at  $T = 313$  K (upper) and  $T = 298$  K (lower).

temperature ( $T_c$ ), critical pressure ( $P_c$ ), and the acentric factor ( $\omega$ ) of the organic solvents and carbon dioxide are from ref 10. For vitamin B<sub>6</sub> the procedure and the method described in ref 7 were used for the evaluation of critical properties and acentric factor. Only one binary parameter  $k_{ij}$  was used for the correlation of the binary solubility of vitamin B<sub>6</sub> in the different organic solvents. The same mixing rule was also applied for the binary system vitamin B<sub>6</sub>–CO<sub>2</sub>: in this case the numerical value of  $k_{ij}$  was calculated by fitting the values of fugacity coefficients at infinite dilution of carbon dioxide in the vitamin reported in ref 11. In the case of the binary systems CO<sub>2</sub>–organic solvent, vapor liquid equilibrium data were used for the calculation of the two binary interaction parameters  $k_{ij}$  and  $l_{ij}$ .

Table 3 reports the numerical values of the binary interaction parameters for the different binary systems necessary to predict the vitamin B<sub>6</sub> behaviors in the ternary systems.

**Particle Size Measurement.** Macroscopic particle size distributions of samples were determined by means of digital image acquisition. Small amounts of each sample were uniformly dispersed on top of glass slide examining at least 500 particles. Acquired pictures were processed with the image analysis program ImageJ.<sup>15</sup> The particle dimension of each sample was determined as length and width (mm).

**Particle Size Estimation.** According to Bristow et al.,<sup>16</sup> the supersaturation is the driving force of the precipitation process, and it is defined as the difference between the real concentration  $C_v$  and the equilibrium one  $C_0$  at a given pressure and temperature. The supersaturation is proportional to the correspondent fugacity coefficient:

$$S = \ln \frac{\varphi(T, P)C_v}{\varphi_0(T, P)C_0} \quad (2)$$

**Table 4. Simulated Yield of Vitamin B<sub>6</sub> Precipitation from Ternary Systems**

vitamin B <sub>6</sub> ternary system with:	T/K	P/MPa	yield %	precipitation/mg
THF–CO <sub>2</sub>	298	5.5	54.8	2.72
	313	7.2	35.7	2.09
acetone–CO <sub>2</sub>	298	5.5	34.1	1.03
	313	7.2	19.4	0.62
EtOH–CO <sub>2</sub>	298	5.5	20.8	2.26
	313	7.2	22.1	2.66
MeOH–CO <sub>2</sub>	298	5.5	38.1	28.3
	313	7.2	34.8	27.6

For low concentrations and a nonvolatile solute, the fugacity effects can be neglected:

$$S = \ln \frac{C_v}{C_0} \quad (3)$$

$$C_0 = m \exp(n \cdot C_{\text{solv}}) \quad (4)$$

where  $m$  and  $n$  are determined by fitting the precipitation curve from the above solubility simulation and  $C_{\text{solv}}$  is the molar ratio of the solvent.

The most important phenomenon affecting the particle size is the primary nucleation mechanism that is promoted at high supersaturation conditions. Nucleation determines both the total number of particles and the final particle size. In the homogeneous one-phase solvent system, the well-known dependency of nucleation rate,  $J$ , on supersaturation,  $S$ , is:

$$\ln \frac{J}{J_{\text{max}}} = AS^{-2} \quad (5)$$

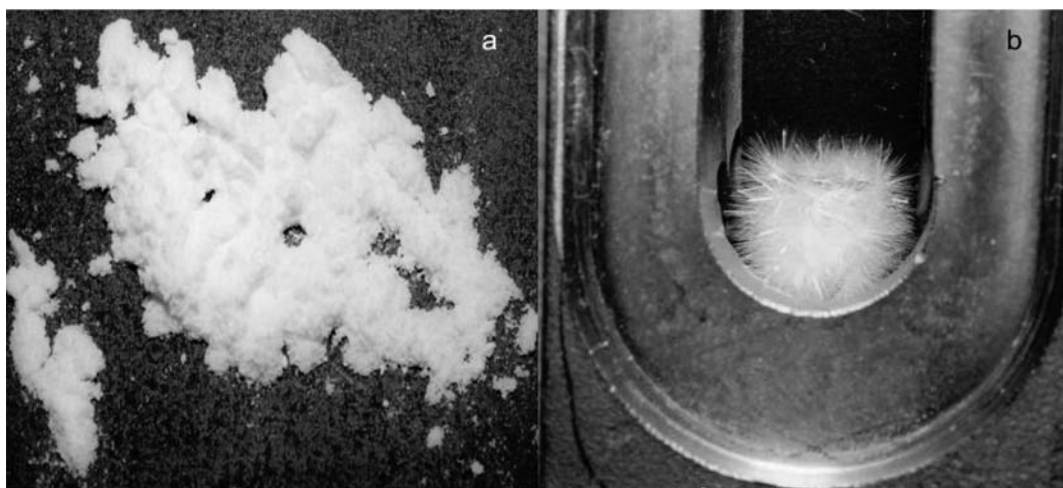


**Figure 2.** Vitamin B<sub>6</sub> before (a) and after (b) precipitation in ethanol solution at the temperature  $T = 313$  K and pressure  $P = 7.2$  MPa.

where  $J_{\max}$  is the pre-exponential nucleation constant and for spherical nuclei the parameter  $A$  is:

$$A = \frac{16\pi\gamma^3 V_{\text{svl}}^2}{3k_B^3 T^3} \quad (6)$$

where  $\gamma$  is the nucleus specific free surface energy and  $k_B$  is the Boltzmann constant.

The crystal growth rate (in the two axes),  $dR_i/dt$ , is described as the screw dislocation equation<sup>17</sup>

$$g_t = \frac{dR_i}{dt} = D_t \left( \frac{S^2}{S_i} \right) \tanh \left( \frac{S_i}{S} \right) \quad (7)$$

where  $R_i$  is the change in crystal size  $D_i$  is a growth constant that is different for each of the axis of the vitamin B<sub>6</sub> crystal ( $i = 1, 2$ , which indicate the major and minor axes, respectively) and that was determined by fitting the experimental particle size data.  $S_i$  is the supersaturation value for which the growth rate dependency switches from first to second order. The theory predicts the particle growth (i.e.,  $dR/dt \propto S^2$ ) when  $S \ll S_i$  (low supersaturation conditions) and when a linear dependence occurs (i.e.,  $(dR/dt) \propto S$ ) in a  $S \ll S_i$  situation.<sup>17</sup>

## RESULTS AND DISCUSSION

**Antisolvent Precipitation.** Vitamin B<sub>6</sub> is in the class of water-soluble vitamins. As a consequence, it is expected that the solubility in  $\text{SCO}_2$  is low, and it was effectively impossible to measure with the normal experimental methods. From the failure of these measurements it is possible to argue that the solubility must be lower than  $10^{-7}$  mole fraction. The only information on the thermodynamic properties for the binary system vitamin B<sub>6</sub>–carbon dioxide are the fugacity coefficients at infinite dilution of carbon dioxide in the vitamin determined at normal pressure.<sup>11</sup> For that reason the binary interaction parameter of the PR EoS for the system was calculated by regression of these data.

For the characterization of the binary systems of the vitamin with the organic solvents the solubility of vitamin B<sub>6</sub> in the solvents was determined at different temperatures and correlated with the PR EoS to obtain for every considered temperature the  $k_{ij}$  interaction parameter between solute and organic solvent.

With these parameters the behavior of the different binary and ternary systems can be predicted.

In this work, triphase phase equilibria have been calculated for different liquid phase concentrations at values of temperature and pressure close to the critical  $\text{CO}_2$  conditions. In fact, the experiments to determine the equilibrium solubility of vitamin B<sub>6</sub> organic solvent solution in  $\text{CO}_2$  were conducted at pressures of 5.5 MPa and 7.2 MPa and temperature of 298 K and 313 K, respectively. The selected organic solvents were characterized by different polarities, like tetrahydrofuran (THF), acetone, ethanol (EtOH), and methanol (MeOH).

Figure 1 depicts the solubility curve simulations of vitamin B<sub>6</sub> in the considered  $\text{CO}_2$ -organic solvent mixtures. The ordinate value  $c$  is:

$$c = \frac{\text{mol}_v}{\text{mol}_{\text{solv}} + \text{mol}_{\text{CO}_2}} \quad (8)$$

and the abscise  $X_{\text{CO}_2}$  is:

$$x_{\text{CO}_2} = \frac{\text{mol}_{\text{CO}_2}}{\text{mol}_{\text{solv}} + \text{mol}_{\text{CO}_2}} \quad (9)$$

where  $\text{mol}_v$  are the moles of vitamin B<sub>6</sub>,  $\text{mol}_{\text{solv}}$  are the moles of organic solvents, and  $\text{mol}_{\text{CO}_2}$  are the moles of  $\text{CO}_2$ .

An increase of  $X_{\text{CO}_2}$  provokes a continuous decrease of vitamin B<sub>6</sub> solubility from the saturation value in pure organic solvent, to the saturation value in pure carbon dioxide. The addition of  $\text{CO}_2$  to saturated vitamin B<sub>6</sub> solutions in the considered organic solvents following the lines depicted in Figure 1, named as ideal dilution lines, denotes the  $\text{CO}_2$  action. The curve over and under this line indicates the  $\text{CO}_2$ -cosolvent and -antisolvent behaviors, respectively.

From these simulations, the mixed actions of  $\text{CO}_2$  that entails both cosolvent and antisolvent seem to be evident.

In all of the investigated ternary systems, except the ones with ethanol, the increased temperature and pressure carry out an enhancement of the  $\text{CO}_2$  cosolvent power.

In Table 4 the predicted yields and corresponding pondering quantities of vitamin B<sub>6</sub> precipitated from the ternary systems are reported. The ternary system of vitamin B<sub>6</sub>– $\text{CO}_2$ –THF at 298 K and 5.5 MPa (Figure 1a) shows the greatest precipitation yield (54.8 %), highlighting the higher THF affinity to  $\text{CO}_2$ , but considering the poor solubility of vitamin B<sub>6</sub> in THF it is



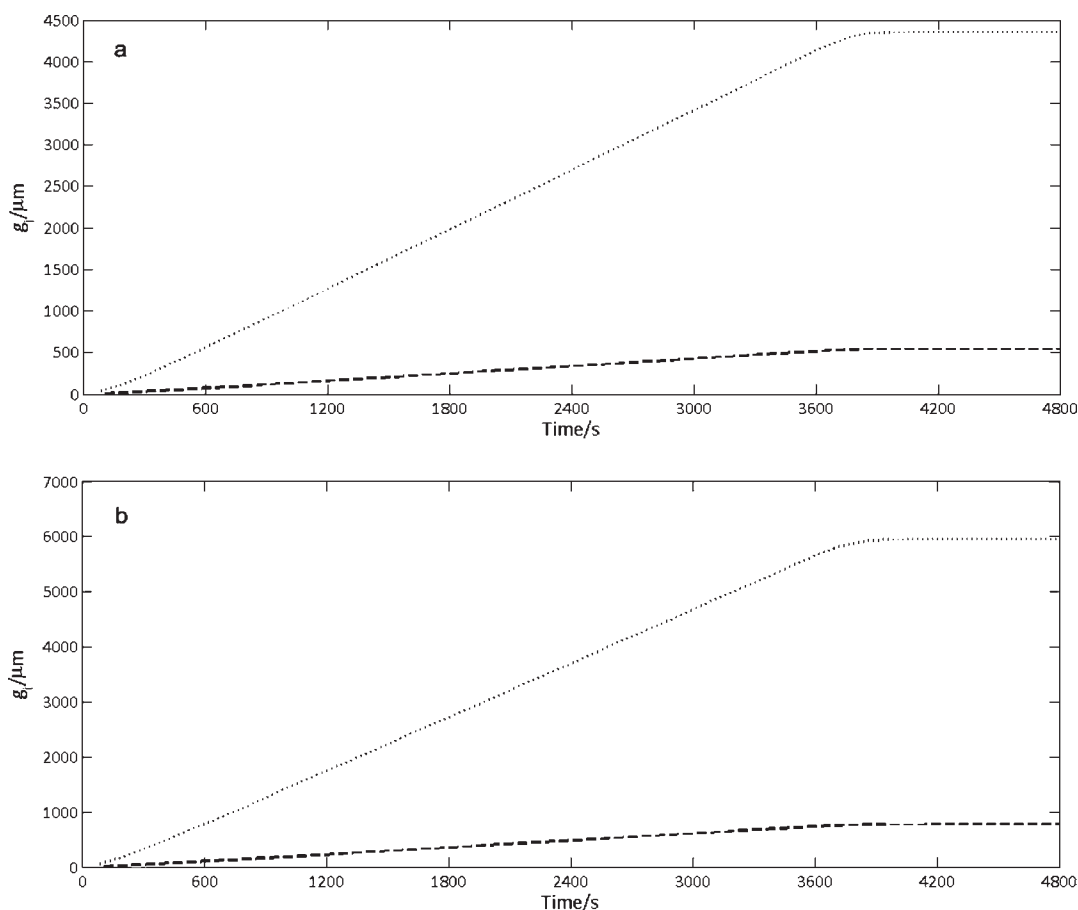


**Figure 3.** Particle size increment along the two axes ( $g_i$ ) versus time of vitamin B<sub>6</sub> with (a) ethanol–CO<sub>2</sub> and (b) methanol–CO<sub>2</sub> at 313 K and 7.2 MPa. The dotted lines depict the major axis. The dashed lines depict the minor axis.

**Table 5. Vitamin B<sub>6</sub> Particle Size Analysis Obtained at Temperature  $T = 313$  K and Pressure  $P = 7.2$  MPa<sup>a</sup> with CO<sub>2</sub>–EtOH (1) and CO<sub>2</sub>–MeOH (2)**

vitamin B <sub>6</sub> -(1)				vitamin B <sub>6</sub> -(2)			
exp <sup>b</sup>		calc <sup>c</sup>		exp <sup>b</sup>		calc <sup>c</sup>	
length/mm	width/mm	length/mm	width/mm	length/mm	width/mm	length/mm	width/mm
3.95 ± 0.71	0.14 ± 0.07	4.31	0.54	5.43 ± 0.65	0.39 ± 0.09	5.95	0.81

<sup>a</sup> Standard uncertainties  $u$  are  $u(T) = 0.1$  K,  $u(P) = 0.07$ . <sup>b</sup> Experimental value (mean ± SD,  $n = 500$ ). <sup>c</sup> Calculated value by means of eq 7.

transduced in a precipitate of 2.72 mg that can be compared to the ethanol systems. The highest quantity of precipitate is obtained with methanol.

In light of these simulations, precipitations of vitamin B<sub>6</sub> were performed only with ethanol and methanol solutions, and Figure 2 depicts the obtained results compared to the starting material. For brevity only the recrystallized Vitamin B<sub>6</sub> in ethanol–CO<sub>2</sub> solution at 313 K and 7.2 MPa is reported.

Simulations of particle size dimension were conducted starting from the equilibrium solubility ( $C_0$ ) of the vitamin B<sub>6</sub> ternary system with EtOH and MeOH and CO<sub>2</sub> at 7.2 MPa and 313 K. Supersaturation  $S$  has been calculated by fitting the solubility curve obtained from the PR EoS.

Vitamin B<sub>6</sub> crystal growth highlights, in both systems, an anisotropic phenomenon in which the substance grows vertically,

in the time, along two axes, suggesting the formation of needle crystals (Figure 3).

At the end of the precipitation (which coincides with the plateau in Figure 3), these results agree with the experimental measurement reported in Table 5, even if there is a certain difference between the calculated and the experimental width. The variation in crystal habit results from the modification of the relative growth rates of crystal faces, which are governed by the degree of supersaturation of the solution, density, and CO<sub>2</sub> flow rate. In general, it is known that, as supersaturation is increased, the crystal form tends to change from granular to needle-like.<sup>18</sup> There is a continuous increase of vitamin B<sub>6</sub> concentration inside the vessel until a critical concentration (supersaturation limit) value is reached for nucleation. Nucleation does not occur until the solute concentration exceeds its  $C_0$  value to a certain limit

dependent on the system. Moreover, in a solution where more solute molecules are present, collisions are more frequent, and nuclei of critical radius can be formed faster.

After the nucleation starts, the accumulating particles become more significant, and the supersaturation inside the vessel increases rapidly. As more particles are formed, the concentration reaches a value close to the  $C_0$  value of 0.779 and 0.652 for EtOH and MeOH systems, respectively, at 313 K and 7.23 MPa ( $X_{CO_2}$ ), and the growth and nucleation rates of the precipitated particles inside the vessel ended. Therefore, monitoring the vitamin B<sub>6</sub> concentration time response provides a useful indicator of the particle formation mechanism inside the collector vessel.

## CONCLUSIONS

Phase equilibrium studies were performed to estimate better operating conditions for the precipitation (GSAS) process. The PR EoS was used to represent solute–solvent antisolvent systems, and it was able to predict ternary behaviors using binary interaction parameters. Moreover, the present EoS is a valid tool to calculate, with the shown screw dislocation equation, the solute crystal growth also along two axes. The supersaturation ratio was directly related to the mean particle size, and it was used to define the mixing conditions in the precipitator chamber and the vitamin B<sub>6</sub> yield in the considered ternary systems. The mechanism of crystallization undergoes a transition across the vitamin B<sub>6</sub>–CO<sub>2</sub>–ethanol and vitamin B<sub>6</sub>–CO<sub>2</sub>–methanol ternary systems solubility curves and is expressed through changes in the surface energy, size, morphology, and agglomeration of the particles.

## AUTHOR INFORMATION

### Corresponding Author

\*E-mail: ireneo.kikic@dicamp.units.it.

### Funding Sources

The authors are very grateful to Beneficentia Stiftung Foundation (Liechtenstein) for financial support.

## REFERENCES

- (1) Bartel, P. R.; Ubbink, J. B.; Delpont, R.; Lotz, B. P.; Becker, P. J. Vitamin B-6 supplementation and theophylline-related effects in humans. *Am. J. Clin. Nutr.* **1994**, *60*, 93–99.
- (2) Ghanshyam, V. J.; Patel, H. A.; Bajaj, H. C.; Jasra, R. V. Intercalation and controlled release of vitamin B6 from montmorillonite–vitamin B6 hybrid. *Colloid Polym. Sci.* **2009**, *287*, 1071–1076.
- (3) Ventosa, N.; Sala, S.; Veciana, J. DELOS process: a crystallization technique using compressed fluids, comparison to the GAS crystallization method. *J. Supercrit. Fluids* **2003**, *26*, 33–45.
- (4) De Gioannis, B.; Gonzalez, A. V.; Subra, P. Antisolvent and cosolvent effect of CO<sub>2</sub> on the solubility of griseofulvin in acetone and ethanol solutions. *J. Supercrit. Fluids* **2004**, *29*, 49–57.
- (5) De. Zordi, N.; Kikic, I.; Moneghini, M.; Solinas, D. Piroxicam solid state studies after processing with SAS technique. *J. Supercrit. Fluids* **2010**, *55*, 340–347.
- (6) Kikic, I.; De Zordi, N.; Moneghini, M.; Solinas, D. Solubility estimation of drugs in ternary systems of interest for the antisolvent precipitation processes. *J. Supercrit. Fluids* **2010**, *55*, 616–622.
- (7) Kikic, I.; Lora, M.; Bertucco, A. Fractional Crystallization By Supercritical Antisolvent Technique: Theory and Experimental Test. *AIChE J.* **1998**, *44*, 2149–2158.
- (8) Prausnitz, J. M.; Lichtenthaler, R. N.; de Azevedo, E. G. *Molecular Thermodynamics of Fluid Phase Equilibria*, 3rd ed.; Prentice-Hall: Englewood Cliffs, NJ, 1999.
- (9) Girolami, G. S. A simple “Back of the Envelope” Method for estimation the densities and molecular volume of liquids and volumes. *J. Chem. Educ.* **1994**, *71*, 962–964.
- (10) Poling, B.; Prausnitz, J. M.; O’Connell, J. P. *The Properties of Gases and Liquids*, 5th ed.; McGraw Hill: New York, 2004.
- (11) Kikic, I.; Alessi, P.; Cortesi, A.; Fabro, L.; Fogar, A. Characterization of Vitamins B and K by Inverse Gas Chromatography (IGC). Annual meeting AIChE, San Francisco, November 2003.
- (12) Kodama, D.; Yagihashi, T.; Hosoya, T.; Kato, M. High pressure vapor-liquid equilibria for carbon dioxide + tetrahydrofuran mixtures. *Fluid Phase Equilib.* **2010**, *297*, 168–171.
- (13) Day, C.; Chang, J.; Chen, C. Correction to phase equilibrium of ethanol + CO<sub>2</sub> and acetone + CO<sub>2</sub> at elevated pressures. *J. Chem. Eng. Data* **1999**, *44*, 365–366.
- (14) Ohgaki, K.; Katayama, T. Isothermal vapor-liquid equilibrium data for the binary systems containing carbon dioxide at high pressures: methanol-carbon dioxide, n-hexane-carbon dioxide, and benzene-carbon dioxide systems. *J. Chem. Eng. Data* **1976**, *21*, 53–55.
- (15) Rasband, W. S. *ImageJ*; U.S. National Institutes of Health: Bethesda, MD, 1997–2005; <http://rsb.info.nih.gov/ij/>.
- (16) Bristow, S.; Shekunov, T.; Shekunov, B. Yu.; York, P. Analysis of the supersaturation and precipitation process with supercritical CO<sub>2</sub>. *J. Supercrit. Fluids* **2001**, *21*, 257–271.
- (17) Dirksen, J. A.; Ring, T. A. Fundamentals of crystallization: kinetic effects on particle size distributions and morphology. *Chem. Eng. Sci.* **1991**, *46*, 2389–2427.
- (18) Halebian, J. K. Characterization of habits and crystalline modification of solids and their pharmaceutical applications. *J. Pharm. Sci.* **1975**, *64*, 1269–1288.